An Implementation of the Quantum Verification of Matrix Products Algorithm

Elton Pinto

1 Introduction

Quantum computing has experienced a recent surge in popularity given the advancements in NISQ machines. Quantum algorithms are known to solve problems like factoring numbers and simulating natural systems more efficiently than a classical computer. Companies such as IBM, Google, and Rigetti have recently built quantum computers that allow researchers to run quantum algorithms on physical hardware. Given these developments, it has become important to survey the feasibility of using quantum computing to solve large-scale problems.

Several studies have experimentally evaluated quantum algorithms on quantum hardware. Mandviwalla et al. evaluated a 4-qubit implementation of Grover search on the IBM-Q quantum processor [12]. Similarly, Acasiete et al. evaluated quantum random walks on graphs with 8 to 16 vertices [14]. However, these studies do not highlight the challenges involved when scaling to larger-sized circuits.

Extensive work has been carried out on developing quantum programming frameworks. IBM has created Qiskit, a Python framework that supports prototyping and executing quantum algorithms on simulators and quantum hardware. ORNL has developed QCOR, a heterogenous classical-quantum framework that aims to use quantum computers as accelerators akin to GPUs [16]. However, little work has been done to evaluate the efficacy of using these frameworks to develop quantum systems.

Our study aims to fill in these gaps by documenting the process of developing an oracle for the Quantum Verification of Matrix Products (QVMP) [4][3] algorithm. This can be tricky to do given the non-deterministic nature of quantum programs and the shortage of formal verification tooling in this space. We implement this algorithm in Qiskit and demonstrate its functionality by running it on the Aer simulator. We report a proof of oracle correctness, circuit metrics (gate count, qubit count, circuit depth), transpilation times, and simulation times.

2 Literature Review

Quantum computing places an emphasis on thinking about how computation is performed physically. It achieves speedup over classical algorithms by exploiting physical phenomenon like entanglement to encode and perform computation. The main promise of the field is that it can offer a non-trivial speedup over classical computing. The algorithm that is frequently brought up to demonstrate this promise is Shor's algorithm. Shor's algorithm provides an exponential speedup over classical algorithms for factoring numbers and is capable of cracking a subset of the widely-used RSA encryption. It achieves this by using the Quantum Fourier Transform (QFT), the quantum analogue of a Fourier transform, to perform phase estimation and order-finding [2].

There are other algorithms like superdense coding, quantum key distribution, and quantum simulation that have potential applications in scientific simulation, machine learning, and cryptography. However, these algorithms tend to require a very large number of qubits to be of practical use. One of the major challenges in developing large-scale multi-qubit systems is error-correction and noise. Before we reach the holy grail of fault-tolerant quantum systems, the field is currently attempting to make use of Noisy Intermediate Quantum Computers (NISQ) to solve problems of important practical use.

Grover's algorithm is a quantum search algorithm that provides an $O(\sqrt{N})$ algorithm for searching through unstructured data, which is a quadratic speed-up over its classical counterpart. It does this by performing multiple Grover iteration steps which constructively amplify states that correspond to search results [2]. A Grover iteration requires a user-defined oracle to function correctly. The job of the oracle is to report back whether an input (encoded as a quantum state) satisfies the search criteria. The core of Grover search is farily straightforward to implement. The main challenge here is efficiently encoding the oracle (which is typically described as a classical decision function) as a quantum circuit. In this study, we try to better understand this challenge by implementing QVMP which uses Grover search (and therefore an oracle) as a sub-routine.

There are two popular algorithms for QVMP. The first algorithm, proposed by Ambainis, Buhrman, Høyer, Karpinski, and Kurur, uses amplitude amplification along with Grover search to look for a sub-matrix that doesn't satisfy the product [3]. This algorithm runs in $O(n^{\frac{7}{4}})$ time and improves upon the optimal classical bound provided by Freivalds [1]. The speedup is obtained because the algorithm makes use of interference to arrive at a result in a smaller number of iterations. However, metrics do not exist for the number of qubits required to implement the oracles for the quantum search algorithms used, and the resources required to carry out operations like multiplying sub-matrices. Further, little research has been done on evaluating the algorithm in a heterogenous classical-quantum setup where quantum computers are used to accelerate certain parts of the algorithm. There exists a 4-qubit physical implementation of Grover search on IBM's quantum processor [12]. This implementation tests IBM quantum computers on Grover's algorithm to investigate the impacts of different circuit and device attributes, and to highlight the current capabilities of the system. This study reports that current quantum computers are able to solve the search problem on very small data sets. This is similar to what our study intends to do, however, it does not investigate the practicality of running algorithms that use Grover search and does not comment on the composability of circuits and how it affects performance and results. The second algorithm, proposed by Buhrman and Spalek, uses quantum random walks to speed up the verification process and runs in $O(n^{\frac{5}{3}})$ time [4].

Quantum random walks are analogous to classical walks, and have a number of applications in quantum programming tasks. For example, they are used in solving the element distinctness problem, in which the goal is to find if there exists a set of M non-distinct elements in a domain of N elements [5]. There have been attempts to run quantum random walks on quantum hardware. Balu et al. implemented an efficient physical realization of a quantum random walk using $log_2(N)$ qubits to represent an N-point lattice [10]. Experimental evaluation was carried out on the IBM-Q five-qubit processor. To overcome resource requirements, they used a continuous time-limit quantum random walk implementation. Acasiete et al. have implemented discrete-time quantum random walks on IBM-Q, and were able to run quantum search based algorithms on graphs with 8 and 16 vertices [14]. They were able to obtain results with 50% fidelity, and claim that the results are more efficient than equivalent classical algorithms.

There exists research on resource estimate quantification and benchmarking for some quantum algorithms. Jaques et al. implemented Grover oracles for key search on AES and LowMC encryption [15]. They lay out a formal description of the oracle, describe a reversible quantum-gate implementation of the AES encryption-decryption algorithm, and estimate the number of Clifford, T, and CNOT gates required for running circuits that can crack AES-128, AES-192, and AES-256. The project uses Q#, a quantum programming language developed by Microsoft. The project reduces the circuit depth of the Grover oracle by using internal parallelization, in which the Grover search instance is run on disjoint subsets of the input domain.

A number of open-source frameworks exist for conducting quantum computing research. IBM provides the Qiskit framework which lets researchers quickly prototype and test algorithms on a simulator, and also run some workloads on a quantum computer, the biggest one being the IBM-Q 16-qubit processor in Melbourne. Fingerhuth et al. have compiled comparisons between Qiskit and other frameworks like Quil, XACC, and ScaffCC [11]. They comment on the programming language choice, documentation, license, and general culture around these communities. However, they do not compare these frameworks based on their performance and ability to execute on quantum hardware. LaRose has compared simulator performance and the quantum compiler of Qiskit and Rigetti [13]. The study does not report which algorithm was used during performance evaluation. Instead, it qualifies a benchmark based on the number of qubits used. ORNL has developed QCOR, which is a heterogenous framework that aims to enable developers to use quantum computers as accelerators, much like GPUs [16]. QCOR doesn't support amplitude amplification, quantum random walks, and basic circuits for performing arithmetic as of now. Support will need to be added to facilitate experimentation using the hybrid classical-quantum programming approach provided by this framework. Salm et al. has worked on a NISQ analyzer that determines the best quantum computer system to run a given workload based on the nature of the quantum algorithm [17]. They believe that this will improve developer experience by obviating the need to understand complicated mathematics to determine the best machine for running a particular quantum programming task. None of the frameworks currently have a working implementation of quantum verification of matrix products which we can use to perform benchmarking.

We believe that it is important to have estimates on how big of an input a concrete implementation of an algorithm can process. We can use such evaluation reports to gauge the current state of quantum computing and suggest areas which need more improvement. Further, we can provide valuable feedback to library authors about features that need to be added to facilitate productive quantum algorithm research.

3 Materials and Methods

This section covers the major components of QVMP, the algorithm itself, implementation details, and experimental setup.

3.1 Grover search

Grover's algorithm is a popular quantum search algorithm. Given an input space of N elements and an oracle U_f, Grover search can find M solution indices in $O(\sqrt{\frac{N}{M}})$ time. For simplicity, we assume that N is a power of 2.

For $M = 1$ Grover search runs in $O(\sqrt{N})$ time, which is a quadratic speedup over the classical algorithm for searching in an unstructured database which takes $O(N)$ time. Therefore, Grover search offers a significant speedup.

The algorithm works by repeatedly applying a Grover operator G to the initial state $H^{\otimes n} |0\rangle^{\otimes n}$:

$$G = (H^{\otimes n}(2|0\rangle\langle 0| - I)H^{\otimes n})U_f = (2|\psi\rangle\langle\psi| - I)U_f \tag{1}$$

It consists of the oracle U_f and a phase shift operator $(2|\psi\rangle\langle\psi| - I)$ known as the diffuser. The specific characteristics of U_f are described in § 3.1.1.

Each iteration can be geometrically viewed as a rotation of the state vector in a plane spanned by the uniform superposition of solutions and non-solutions. After the application of U_f, the diffuser rotates the state vector towards the superposition of solutions. The number of such iterations can be shown to be $O(\sqrt{\frac{N}{M}})$. Therefore, in order to use Grover's algorithm, one needs to know the exact number of solutions M in the search space.

The Grover operator circuit is summarized in Fig. 1.

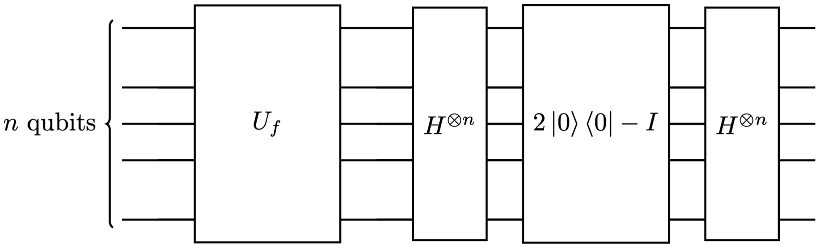

Figure 1: Grover operator circuit

3.1.1 Grover Oracles

The oracle U_f used in Grover's algorithm can be viewed as black box that knows how to recognize solutions in the search problem. Let us say we are given a function f which takes an input $x \in N$ and returns 1 if x is a solution to the search problem, and 0 otherwise. Then, the action of U_f can be written as:

$$U_f|x\rangle \mapsto (-1)^{f(x)}|x\rangle \tag{2}$$

Note how the oracle only applies a phase shift to solutions of the search space.

The above oracle is commonly implemented by encoding f in a quantum circuit that flips a target qubit $|y\rangle$ for all inputs x that are a solution to the search problem. We obtain the phase shift by initializing the target qubit to the $|-\rangle$ state.

3.2 Amplitude Amplification

Amplitude amplification is a generalization of the Grover operator G. Instead of wrapping Hadamard gates H around the diffuser, we now use an arbitrary unitary U.

$$U(2\,|0\rangle\,\langle 0| - I)U^{\dagger}O \tag{3}$$

The oracle O behaves in the same way as described in § 3.1.1. The unitary can be thought of as a quantum subroutine A that performs a series of quantum operations without making measurements.

3.3 Quantum Verification of Matrix Products

Given three square matrices A, B, and C of size n, the verification of matrix products (VMP) decides if $AB = C$. Freivalds describes a classical algorithm which can run in $O(n^2)$ time.

In this paper, we implement the recursive Grover search based quantum VMP by Ambainis et al. [3]. The algorithm proceeds by first partitioning B and C into submatrices B_i and C_i of size $n \times \sqrt{n}$ respectively. It is easy to observe that $AB = C$ iff $AB_i = C_i\ \forall i$. Now, perform amplitude amplification over the following subroutine: pick a random vector x, classically compute $y = B_i x$ and $z = C_i x$, and verify the product $Ay = z$. The verification is done using a Grover search where the search space is the set of row indices and the oracle verifies if the inner product between the row and the vector matches the output.

The verification oracle takes $O(n)$ time. Therefore, each Grover iteration runs in $O(n^{\frac{3}{2}})$ time. We need to run $\sqrt{\frac{n}{\sqrt{n}}} = n^{\frac{1}{4}}$ iterations of amplitude amplification. Therefore, the overall running time of the algorithm is $O(n^{\frac{7}{4}})$.

The algorithm is summarized in Alg. 1.

Algorithm 1 Quantum VMP using Grover Search [8]

```
Input:  $n \times n$ matrices $A, B, C$
Output:  1 if $AB = C$ and 0 otherwise
Procedure:
  1. Partition $B$ and $C$ into sub-matrices of size $n \times \sqrt{n}$
  2. Perform amplitude amplification for $n^{\frac{1}{4}}$ iterations using this subroutine:
      (a) Pick a random vector $x$ of size $\sqrt{n}$
      (b) Classically compute $y = B_i x$ and $z = C_i x$
      (c) Using Grover search with $\sqrt{n}$ iterations, find a row of index $j$ such that $(Ay \neq z)_j$
  3. XOR the sub-results
```

3.4 Implementation

We implement QVMP in Qiskit, a popular open-source quantum computing platform developed by IBM. Qiskit uses Python as the host language and has a large libary of utilities that allow developers to compose non-trivial circuits. It ships with a transpiler and several backends capable of running circuits on simulators and quantum hardware.

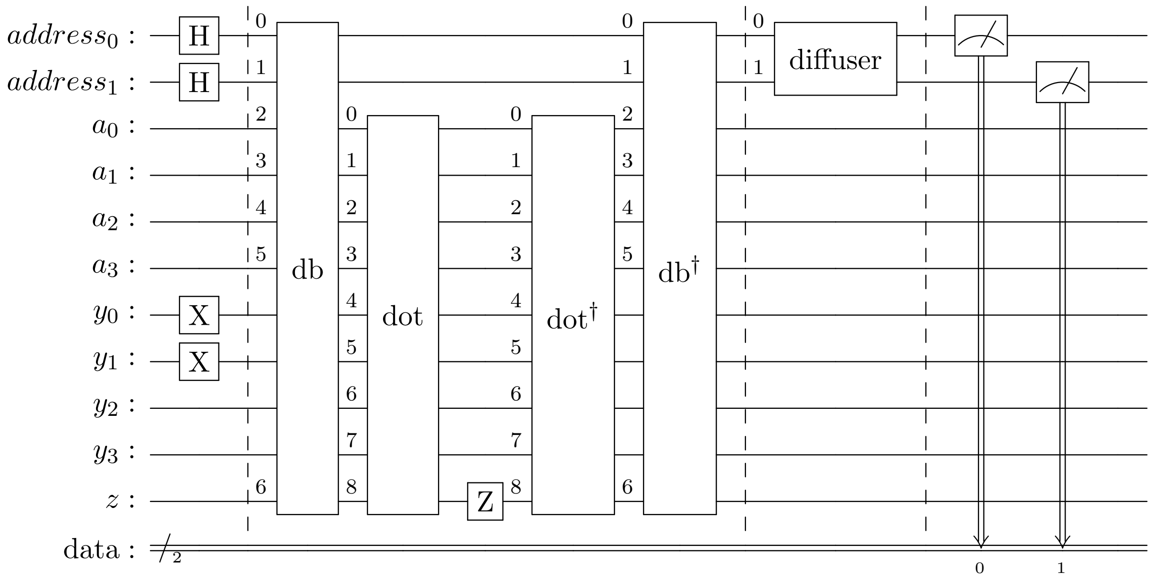

Figure 2: QVMP circuit for a 4 × 4 matrix A performing one iteration

We restrict our implementation to only support binary matrices. Remaining details can be found in § 4.

3.5 Experimental Setup

The experiments were run on an AMD EPYC 7502 32-Core Processor, 2.5 GHz, 128 CPUs. The source code is available at `https://github.com/1ntEgr8/qvmp`.

4 Implementation

This section describes and analyzes the implementation of the quantum portion of the algorithm (steps 2 and 2.3 of Alg. 1).

Fig. 2 shows an example circuit that performs one iteration of the Grover operator used in step 2.3. The sub-circuits used are Quantum Read-Only Memory (QROM) [9] (denoted by *db*), out-of-place inner product (denoted by *dot*), and diffuser.

Amplitude amplification (step 2) is carried out by first running Grover search (step 2.3) and then appending a diffuser circuit. Describing it in terms of the notation developed in § 3.2, U would be the Grover search circuit.

To perform Grover search, we need to implement an oracle. The QVMP oracle is a blackbox that checks if $(Ay - z)_j \neq 0$ where A, y, z, and j are as defined in Alg. 1. Qiskit offers the `classical_function` decorator which allows you to describe Grover oracles classically. However, the programs are restricted to using boolean operators and do not have support for higher-level primitives like matrices, vectors, and related operations (which we need). This means that we needed to hand-code the oracle from scratch.

$$A = \begin{bmatrix} 0 & 1 & 0 & 1 \\ 1 & 1 & 1 & 0 \\ 1 & 0 & 0 & 1 \\ 1 & 0 & 1 & 0 \end{bmatrix}$$

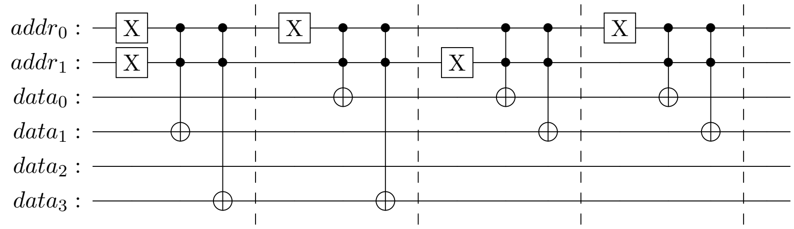

Figure 3: QROM encoding of a 4 × 4 matrix A

The QVMP oracle needs to perform the following steps:

- Encode the inputs A, y, and z
- Calculate the inner product Ay and for each row index j compute $(Ay \neq z)_j$
- Mark a qubit if the constraint is satisfied (thereby obtaining a marking oracle)
- Convert the marking oracle into a phase oracle
- Uncompute on the ancilla qubits

We encode A and z using QROM. y is encoded using a bit-to-qubit encoding. The inner product is computed using an out-of-place inner product circuit. We use a Z gate to perform the phase-flip on the marked qubit, which correctly converts our oracle from marking to phase (see § 4.4). Finally, we uncompute the inner-product and QROM circuits to return the ancilla qubits to their original state.

4.1 QROM

QROM can encode an $n \times m$ binary matrix using $m + \log_2(n)$ qubits. This is quadratic improvement over a naive bit-to-qubit encoding where each binary value is assigned to a qubit (resulting in $O(n^2)$ space-complexity).

QROM takes in a row index encoded as a binary value using $log_2(n)$ address qubits encodes the data for the row in m data qubits. This is done by partitioning the circuit into $log_2(n)$ chunks, where each chunk corresponds to an address. Using multi-controlled NOT gates it selectively updates the data qubits corresponding to the input address with the corresponding values.

Since this is a quantum circuit, we can use superposition to pass in multiple row-indices through the address qubits and read multiple rows. The caveat is, of course, that we can only measure one of the rows. Nonetheless, we can still exploit this feature of QROMs to perform the same computation on multiple rows and boost the probability of measure a particular row through amplitude amplification for example.

Fig. 3 shows a QROM circuit encoding a 4 × 4 matrix A.

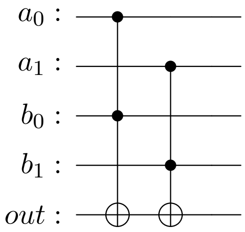

Figure 4: Inner product circuit for 2-D vectors

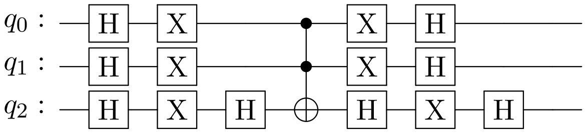

Figure 5: Diffuser running on three qubits

4.1.1 QROM in QVMP

We use QROM to encode A and z (concatenated as an $n \times (m+1)$ matrix. There is, however, the question of why we can't encode y using QROM as well. The answer is that we will not be able to perform the inner product between A_j and y using such a scheme. This is because to perform the inner product we need a single row of A but **all** the rows in the vector y because of the way matrix multiplication works. z can be encoded using QROM since we only need the value of z_j.

4.2 Inner Product (out-of-place)

The inner product circuit, as the name suggests, computes the inner product between two binary vectors encoded using bit-to-qubit encoding. Addition and multiplication are as those typically defined for the field F_2. The circuit consists of a series of Tofolli gates controlled on the corresponding inputs with a single target qubit different from the input qubits (hence out-of-place).

Fig. 4 shows an inner-product circuit between 2-D vectors.

4.2.1 Inner Product in QVMP

We use the inner product circuit to compute $(Ay)_j$. Note that we are using z as the target qubit. This serves the purpose of both calculating $(Ay)_j$ and comparing it to z. The output of z will be 0 if they don't match and 1 if they do. This is precisely why performing a Z gate on z is sufficient to convert our oracle from marking to phase.

4.3 Diffuser

The diffuser is implemented exactly as described in § 3.1. Fig. 5 shows a diffuser running on three qubits.

4.4 Oracle correctness

Claim. Given a superposition of row indices $addr$, an $n \times m$ binary matrix A, and m-dimensional binary vectors y and z, the QVMP oracle will flip the phase of the row indices j which satisfy $(Ay \neq z)_j$ and leave the ancilla qubits unchanged.

Proof. Let $a_1, a_2, \ldots, a_k$ be row indices selected from the set $\{0, \ldots, n-1\}$ for some $0 \leq k \leq n$.

The initial state of the circuit (after encoding y) is

$$\psi_0 = (\alpha_1 |a_1\rangle + \alpha_2 |a_2\rangle + \ldots + \alpha_k |a_k\rangle) |0\rangle^{\otimes m} |y\rangle |0\rangle$$

where $\alpha_i \in \mathbb{C}$ are the amplitudes.

Applying the oracle (using the notation of Fig. 2),

$$\begin{aligned}
\psi_0 &\xrightarrow{db} (\alpha_1 |a_1\rangle |A_{a_1}\rangle |z_{a_1}\rangle + \ldots + \alpha_k |a_k\rangle |A_{a_k}\rangle |z_{a_k}\rangle) |y\rangle \\
&\xrightarrow{dot} (\alpha_1 |a_1\rangle |A_{a_1}\rangle |z_{a_1} \oplus (Ay)_{a_1}\rangle + \ldots + \alpha_k |a_k\rangle |A_{a_k}\rangle |z_{a_k} \oplus (Ay)_{a_k}\rangle) |y\rangle \\
&\xrightarrow{Z} ((-1)^{z_{a_1} \oplus (Ay)_{a_1}} \alpha_1 |a_1\rangle |A_{a_1}\rangle |z_{a_1} \oplus (Ay)_{a_1}\rangle + \ldots + (-1)^{z_{a_k} \oplus (Ay)_{a_k}} \alpha_k |a_k\rangle |A_{a_k}\rangle |z_{a_k} \oplus (Ay)_{a_k}\rangle) |y\rangle \\
&\xrightarrow{dot^\dagger} ((-1)^{z_{a_1} \oplus (Ay)_{a_1}} \alpha_1 |a_1\rangle |A_{a_1}\rangle |z_{a_1}\rangle + \ldots + (-1)^{z_{a_k} \oplus (Ay)_{a_k}} \alpha_k |a_k\rangle |A_{a_k}\rangle |z_{a_k}\rangle) |y\rangle \\
&\xrightarrow{db^\dagger} ((-1)^{z_{a_1} \oplus (Ay)_{a_1}} \alpha_1 |a_1\rangle + \ldots + (-1)^{z_{a_k} \oplus (Ay)_{a_k}} \alpha_k |a_k\rangle) |0\rangle^{\otimes m} |y\rangle |0\rangle
\end{aligned}$$

$(-1)^{z_{a_i} \oplus (Ay)_{a_k}}$ equals -1 if $(Ay \neq z)_{a_k}$. It is 1 otherwise.

This proves the claim. □

5 Results

QVMP specifies that we run $N = n^{\frac{1}{4}}$ iterations of the Grover operator regardless of the number of solutions m. The optimal number of iterations $N_{\text{optimal}} \approx \frac{\pi}{4}\sqrt{\frac{n}{m}} \leq N, \forall n$. We can use either number of iterations to perform QVMP. The former requires performing amplitude amplification and while the latter doesn't. We explicitly mention which one we are using when discussing our results.

The simulations were carried out using the Aer backend provided by Qiskit. Aer supports different simulation methods, two of which are statevector and matrix product state (MPS). The statevector method performs a dense statevector simulation of the quantum state. The memory requirements for this method scale exponentially with the number of qubits. We were able to simulate circuits containing up to 32 qubits with this method before hitting memory limits. The MPS method allows for more efficient operations on circuits with relatively low entanglement. We were able to simulate the entirety of our desired input space using this method.

5.1 Functionality

Fig. 6 demonstrates that our implementation is able to find the row indices under both N and N_{optimal} iterations.

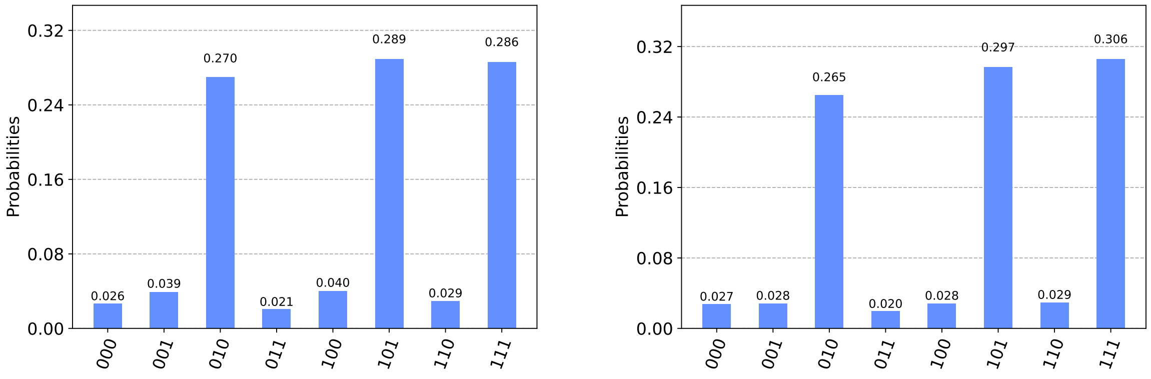

(a) Using N_{optimal}

(b) Using N

Figure 6: Histogram showing the probability distribution of measuring the address qubits of the QVMP circuit for an 8×8 matrix with $(Ay \neq z)_j$ for $j \in \{2, 5, 7\}$

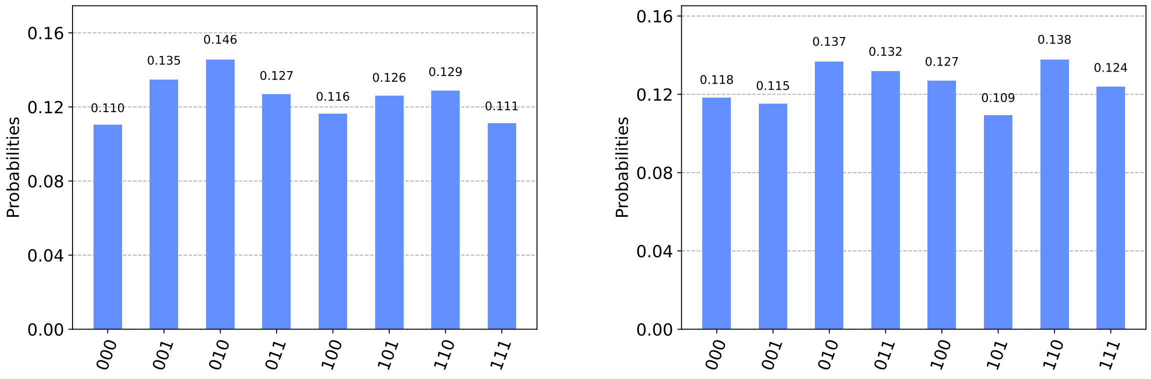

(a) Using N_{optimal}

(b) Using N

Figure 7: Histogram showing the probability distribution of measuring the address qubits of the QVMP circuit for an 8×8 matrix with no j satisfying $(Ay \neq z)_j$

Fig. 7 demonstrates the case when no solutions are present. There is an equal probability of measuring any of the row indices.

As the number of iterations increases, the amplitudes start oscillating around the optimal value. We define the period to be the number of oscillations between optimals. Fig. 8 and Fig. 9 demonstrate cases when the algorithm fails to find a solution even when one exists. The former occurs when N is not equal to $\lfloor k * \text{period} \rfloor$ for some integer k. For example, in Fig. 8, the period ≈ 1.313, $N = 4$, and the sequence of periods is $1, 2, 3, 5, \ldots$. We can handle this by hypertuning the number of iterations to be close to the optimal. The latter occurs when the number of optimal Grover iterations rounds down to zero. We can handle this by running the algorithm on the dual problem, i.e., finding j where $(Ay = z)_j$.

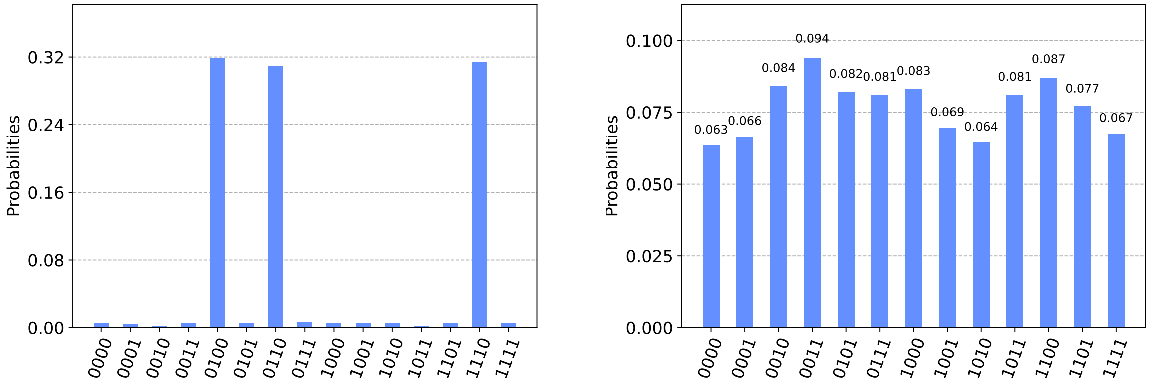

(a) Using $N_{\text{optimal}} = 1$

(b) Using $N = 4$

Figure 8: **Failure case** Histogram showing the probability distribution of measuring the address qubits of the QVMP circuit for a 16×16 matrix with $(Ay \neq z)_j$ $j \in \{1, 4, 5\}$. $N \neq \lfloor k * \text{period} \rfloor$

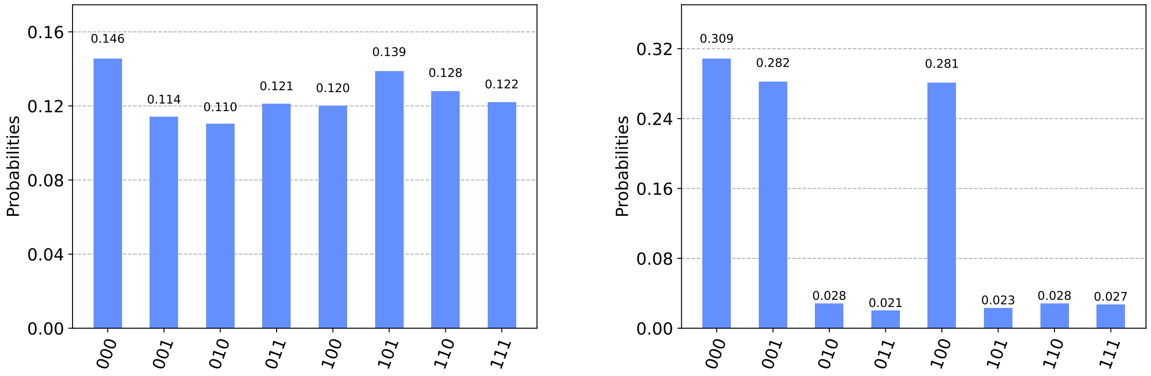

(a) Using $N_{\text{optimal}} = 0$

(b) Using $N = 2$

Figure 9: **Failure case** Histogram showing the probability distribution of measuring the address qubits of the QVMP circuit for an 8×8 matrix with $(Ay \neq z)_j$ for $j \in \{2, 3, 5, 6, 7\}$. $N_{\text{optimal}} = 0$

5.2 Circuit Metrics

Table 1 reports circuit metrics (gate count, circuit depth, qubit count) measured when using the MPS and statevector methods for the Grover search portion of QVMP (step 2.3 in Alg. 1. The metrics are reported on circuits that used N_{optimal} iterations.

The qubit count is precisely $m + \log_2(n) + n + 1$ for an $n \times m$ matrix. In other words, it is linear in the size of the input. Circuit depth is an important metric because it impacts both transpilation time and fidelity of the output.

Fig. 10 shows the circuit depths before and after transpilation. When using the statevector method we see a small decrease in the circuit depth. Using MPS, on the other hand, results in two to three orders of magnitude more gate count and circuit depth. The additional gates for MPS seem to be mostly CNOTs. A cursory look at a function call profile reveals that transpilation for MPS

Dimension	Mismatches	ccx	cx	x	h	z	u1	u2	u3	Grover iterations	Depth	Qubits	Total gates
(4, 4)	1	30	1	11	2	1	2	2	0	1	44	11	49
(16, 4)	2	16	6220	68	176	2	5216	1564	3	2	10585	13	13265
(16, 8)	2	32	10108	69	284	2	8460	2536	3	2	16993	21	21494
(32, 4)	2	24	42060	204	461	3	42037	504	6	3	69510	14	85299
(32, 8)	1	64	91408	272	997	4	91377	1056	8	4	150375	22	185186
(32, 32)	3	128	185912	151	2025	2	185897	2052	4	2	303901	70	376171
(64, 8)	3	48	300324	401	1602	3	300315	1632	4	3	497172	23	604329
(64, 16)	2	128	786960	538	4190	4	786948	4232	5	4	1300351	39	1583005
(64, 64)	3	384	2329596	432	12396	3	2329587	12426	4	3	3843672	135	4684828

(a) MPS

Dimension	Mismatches	ccx	cx	x	h	z	u1	u2	u3	Grover iterations	Depth	Qubits	Total gates
(4, 4)	1	30	1	11	2	1	2	2	0	1	44	11	49
(16, 4)	2	16	0	75	4	2	3	12	1	2	261	13	113
(16, 8)	2	32	0	76	4	2	3	12	1	2	385	21	130
(32, 4)	2	24	0	208	5	3	4	24	2	3	684	14	270
(64, 8)	3	48	0	405	6	3	4	30	2	3	2040	23	498
(64, 8)	1	96	0	801	6	6	7	60	5	6	4077	23	981

(b) Statevector

Table 1: Circuit metrics for MPS and statevector simulation methods on select dimensions. Depth and total gates were measured after transpilation.

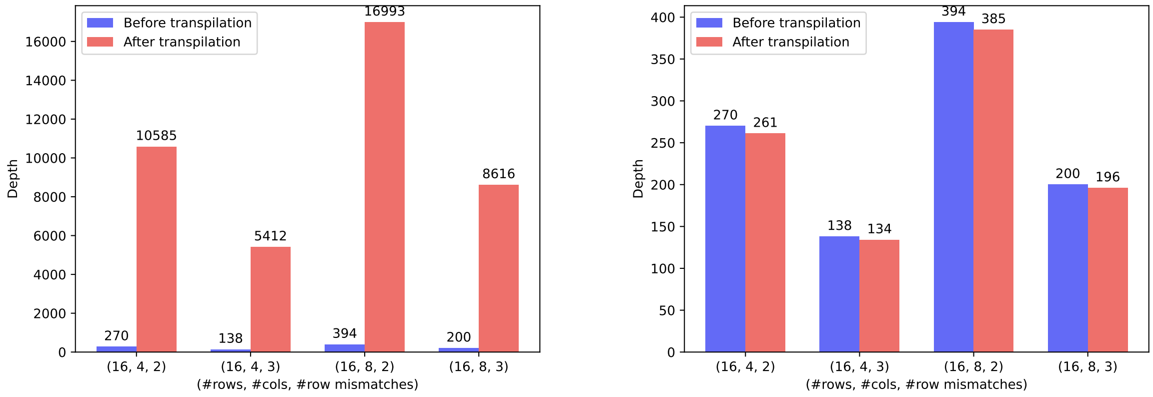

(a) MPS

(b) Statevector

Figure 10: Comparison of circuit depth before/after transpilation on select dimensions

spends most of its time performing SWAPs (which consist of CNOTs). Future work will look into investigating why these SWAPs are performed even though the target architecture (which is Aer in our case) is fully-connected.

From these Aer simulations, we conclude that it is possible to run QVMP on up to 32 qubits using NISQ hardware.

5.3 Transpilation and Simulation

Fig. 11 showcases how transpilation time and simulation time change as the circuit depth increases. We observe opposite trends. MPS seems to be spending more time on transpilation while its simulation time remains mostly constant. Statevector, on the other hand, spends more time during

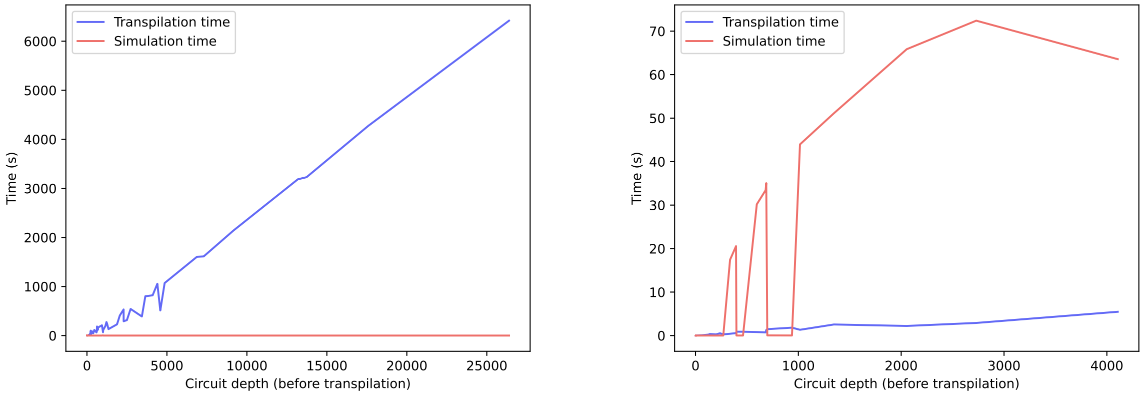

(a) MPS

(b) Statevector

Figure 11: Circuit depth vs Transpilation/Simulation time

simulation with transpilation time growing at a slow rate. We observe this trend mainly due to the gate explosion described in § 5.2.

5.4 Challenges

Implementing and debugging Grover oracles in Qiskit is error-prone. The library does not offer support for encoding matrices into quantum circuits and performing operations on them. The choice of encoding scheme is left to the programmer. This can slow development time since programmers are now forced to work at lower level of abstraction than desired. Debugging quantum circuits can be tricky. Consider the following scenario. You've implemented a Grover oracle. After running the simulation, however, you observe that your circuit is not amplifying the correct states. This error could be due to a number of reasons: ancilla qubits may have become entangled with the input qubits or diffusion might have been applied on the wrong set of qubits, to name a few. Debugging this in Qiskit involves inserting statevector probes to view the state of the quantum system and then identify any discrepancies. While not difficult to do, it can eat up developer time. We believe that Grover oracle synthesis should be automated to a high-degree. When possible, such a system should be able to produce a proof of correctness.

There is also the challenge of scaling quantum circuit development. Transpilation and simulation times can become bottlenecks in the iteration cycle.

6 Conclusion

In this study we present an implementation of QVMP in Qiskit. We reported circuit metrics (gate count, depth, qubit count) as well as transpilation and simulation times. While QVMP can be simulated (and even run) on moderately-sized inputs, it cannot, with current hardware, scale to a degree where we can observe any quantum advantage. We demonstrate that the simulation method selected can have a noticeable impact on depth of the circuit, the effects of which trickle into transpilation and simulation time.

Future work in this space involves extending existing reversible compilers (like REVS [7] and a

```
(* Example program describing the QVMP oracle *)

[@@oracle]
let find_row_mismatch a y z =
  find_idx (fun idx value -> value <> z[idx]) (a * y)
```

Figure 12: High-level description of QVMP in the ML dialect. @@oracle is an attribute specifying that the expression that follows is an oracle that can be compiled to a reversible circuit

subset of Quipper [6]) to support higher-level programming constructs like lists, records, and multi-dimensional arrays. This will allow programmers to specify oracles as high-level classical decision functions without having to think about encoding schemes, thereby raising the level of abstraction which can boost productivity. Fig. 12 demonstrates such a description for QVMP.

Another direction involves investigating the gate and circuit depth explosion observed when using the MPS simulation method. Cursory investigation has revealed that the transpiler is inserting multiple SWAP gates despite the target architecture being fully-connected.

Finally, we also wish to explore the space of more efficient encodings of matrices and related operations to cut down on qubit counts.

Bibliography

[1] Rūsiņš Freivalds. “Fast probabilistic algorithms”. In: *International Symposium on Mathematical Foundations of Computer Science*. Springer, 1979, pages 57–69.

[2] Michael A Nielsen and Isaac L Chuang. *Quantum computing and quantum information*. Cambridge University Press, 2000.

[3] Andris Ambainis et al. “Quantum matrix verification”. In: *Unpublished manuscript* (2002).

[4] Harry Buhrman and Robert Spalek. “Quantum Verification of Matrix Products”. In: *arXiv:quant-ph/0409035* (July 6, 2005). arXiv: `quant-ph/0409035`.

[5] Andris Ambainis. “Quantum Walk Algorithm for Element Distinctness”. In: *SIAM Journal on Computing* 37.1 (Jan. 2007), pages 210–239.

[6] Alexander S Green et al. “Quipper: a scalable quantum programming language”. In: *Proceedings of the 34th ACM SIGPLAN conference on Programming language design and implementation*. 2013, pages 333–342.

[7] Matthew Amy, Martin Roetteler, and Krysta M Svore. “Verified compilation of space-efficient reversible circuits”. In: *International Conference on Computer Aided Verification*. Springer. 2017, pages 3–21.

[8] Adetokunbo Adedoyin et al. “Quantum algorithm implementations for beginners”. In: *arXiv preprint arXiv:1804.03719* (2018).

[9] Ryan Babbush et al. “Encoding electronic spectra in quantum circuits with linear T complexity”. In: *Physical Review X* 8.4 (2018), page 041015.

[10] Radhakrishnan Balu, Daniel Castillo, and George Siopsis. “Physical realization of topological quantum walks on IBM-Q and beyond”. In: *Quantum Science and Technology* 3.3 (2018), page 035001.

[11] Mark Fingerhuth, Tomáš Babej, and Peter Wittek. “Open source software in quantum computing”. In: *PLOS ONE* 13.12 (Dec. 20, 2018). Edited by Leonie Anna Mueck, e0208561.

[12] Aamir Mandviwalla, Keita Ohshiro, and Bo Ji. “Implementing Grover’s Algorithm on the IBM Quantum Computers”. In: *2018 IEEE International Conference on Big Data (Big Data)*. 2018 IEEE International Conference on Big Data (Big Data). Seattle, WA, USA: IEEE, Dec. 2018, pages 2531–2537.

[13] Ryan LaRose. “Overview and Comparison of Gate Level Quantum Software Platforms”. In: *Quantum* 3 (Mar. 25, 2019), page 130.

[14] Frank Acasiete et al. “Implementation of quantum walks on IBM quantum computers”. In: *Quantum Information Processing* 19.12 (2020), pages 1–20.

[15] Samuel Jaques et al. “Implementing Grover Oracles for Quantum Key Search on AES and LowMC”. In: *Advances in Cryptology – EUROCRYPT 2020*. Edited by Anne Canteaut and Yuval Ishai. Volume 12106. Series Title: Lecture Notes in Computer Science. Cham: Springer International Publishing, 2020, pages 280–310.

[16] Tiffany M. Mintz et al. “QCOR: A Language Extension Specification for the Heterogeneous Quantum-Classical Model of Computation”. In: *ACM Journal on Emerging Technologies in Computing Systems* 16.2 (Apr. 30, 2020), pages 1–17.

[17] Marie Salm et al. “The NISQ Analyzer: Automating the Selection of Quantum Computers for Quantum Algorithms”. In: *Service-Oriented Computing*. Edited by Schahram Dustdar. Volume 1310. Series Title: Communications in Computer and Information Science. Cham: Springer International Publishing, 2020, pages 66–85.